

Design of passive interconnections in tall buildings subject to earthquake disturbances to suppress inter-storey drifts

Yamamoto, Kaoru

Department of Electrical and Computer Engineering, University of Minnesota

Smith, M. C.

Department of Engineering, University of Cambridge

<https://hdl.handle.net/2324/4784739>

出版情報 : Journal of Physics: Conference Series. 744 (012063), 2016. IOP Publishing

バージョン :

権利関係 : Creative Commons Attribution International



PAPER • OPEN ACCESS

Design of passive interconnections in tall buildings subject to earthquake disturbances to suppress inter-storey drifts

To cite this article: K Yamamoto and MC Smith 2016 *J. Phys.: Conf. Ser.* **744** 012063

View the [article online](#) for updates and enhancements.

You may also like

- [Dynamic modelling and control of shear-mode rotational MR damper for mitigating hazard vibration of building structures](#)
Yang Yu, Sayed Royel, Yancheng Li et al.
- [A hybrid MRE isolation system integrated with ball-screw inerter for vibration control](#)
Shida Jin, Shuaishuai Sun, Jian Yang et al.
- [High-strength steel frames with SMA connections in self-centring energy-dissipation bays: insights and a multimodal nonlinear static procedure](#)
Ke Ke, Michael C H Yam, Huanyang Zhang et al.



The Electrochemical Society
Advancing solid state & electrochemical science & technology

242nd ECS Meeting

Oct 9 – 13, 2022 • Atlanta, GA, US

Extended abstract submission deadline: April 22, 2022

Connect. Engage. Champion. Empower. Accelerate.

MOVE SCIENCE FORWARD



Submit your abstract



Design of passive interconnections in tall buildings subject to earthquake disturbances to suppress inter-storey drifts

K Yamamoto¹ and MC Smith²

¹ Department of Electrical and Computer Engineering, University of Minnesota, Minneapolis, MN 55455, USA

² Department of Engineering, University of Cambridge, Cambridge CB2 1PZ, UK

E-mail: ¹kyamamot@umn.edu, ²mcs@eng.cam.ac.uk

Abstract. This paper studies the problem of passive control of a multi-storey building subjected to an earthquake disturbance. The building is represented as a homogeneous mass chain model, i.e., a chain of identical masses in which there is an identical passive connection between neighbouring masses and a similar connection to a movable point. The paper considers passive interconnections of the most general type, which may require the use of inerters in addition to springs and dampers. It is shown that the scalar transfer functions from the disturbance to a given inter-storey drift can be represented as complex iterative maps. Using these expressions, two graphical approaches are proposed: one gives a method to achieve a prescribed value for the uniform boundedness of these transfer functions independent of the length of the mass chain, and the other is for a fixed length of the mass chain. A case study is presented to demonstrate the effectiveness of the proposed techniques using a 10-storey building model. The disturbance suppression performance of the designed interconnection is also verified for a 10-storey building model which has a different stiffness distribution but with the same undamped first natural frequency as the homogeneous model.

1. Introduction

One of the main objectives for seismic design is to limit the inter-storey drifts in response to disturbances. For this purpose, the installation of passive control devices between floors is widely adopted [1–3]. The basic principle of control using inter-storey devices, i.e., devices interconnecting neighbouring storeys, is to increase the energy dissipation capability of the structure. To this end, dampers of various types are frequently employed. Other devices such as inerters [4] may also be incorporated to enhance the performance in addition to springs and dampers. The *inertor* is a mechanical two-terminal, one-port device with the property that the applied force at the terminals is proportional to the relative acceleration between the terminals, i.e., $F = b(\ddot{v}_2 - \ddot{v}_1)$ where b is the constant of proportionality called the *inertance* which has units of kilograms [4] and v_1, v_2 are the terminal velocities.

Applications of inerters for building vibration suppression have been extensively studied in recent years, e.g., [5–10]. These design methods, however, may only be applicable to a specific device configuration. Although the problem setup considered in [11, 12] is applicable to more general configurations, the optimisation algorithms used in these articles resulted in a design



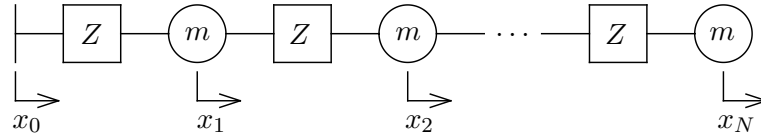


Figure 1. Chain of N masses m connected by a passive mechanical impedance $Z(s)$ (admittance $Y(s) = Z(s)^{-1}$), and connected to a movable point x_0 .

which gives a large resonance peak outside of the frequency range considered. This suggests that more careful analysis will be required for incorporating inerters in buildings.

This paper proposes a systematic and intuitive design methodology which covers any layouts consisting of springs, dampers and inerters. In particular, we study the scalar transfer functions from the movable point displacement x_0 to a given individual intermass displacement (an interstorey drift in the building application) in a chain of N identical masses with identical passive interconnection (Fig. 1). An idealised model for analysing the seismic response of a building which takes this form is a shear-type building model. We refer to this model as “the homogeneous mass chain”, or simply “the mass chain”. The authors have shown in [13] that the scalar transfer functions from the disturbance to a given intermass displacement can be represented as complex iterative maps. Using these expressions, the present paper proposes two graphical approaches: one gives a method to achieve a prescribed value for the uniform boundedness of these transfer functions independent of the length of the mass chain, and the other is for a fixed length of the mass chain. More specifically, we firstly introduce a graphical approach to select the interconnection impedance that achieves a good disturbance rejection performance in an arbitrary length of the mass chain. This is motivated by an increasing trend to build ever taller buildings. Secondly we propose a design methodology for a fixed length of the mass chain subject to a frequency-weighted disturbance. It may be expected that a better disturbance rejection performance is achievable when we know the number of the storeys of the building to be designed, which is often the case in practice, and characteristics of the disturbance are also incorporated in the design process. For this aim, a graphical technique is proposed. We employ a weighting function on the earthquake disturbance that is based on the well-known Clough-Penzien and Kanai-Tajimi acceleration filter. A case study is presented to demonstrate the effect of the proposed techniques using a 10-storey building model. The disturbance suppression performance of the designed interconnection is also verified for a 10-storey building model which has a different stiffness distribution but with the same undamped first natural frequency as the homogeneous model.

2. Background on passive mechanical networks

A mechanical one-port network with force-velocity pair (F, v) is *passive* if for all square integrable pairs $F(t)$ and $v(t)$ on $(-\infty, T]$, $\int_{-\infty}^T F(t)v(t)dt \geq 0$ [14]. For a linear time-invariant network the impedance $Z(s)$ is defined by the ratio $\hat{v}(s)/\hat{F}(s)$ where $\hat{\cdot}$ denotes the Laplace transform, and $Y(s) = Z(s)^{-1}$ is called the admittance. Such a network can be shown to be passive if and only if $Z(s)$ or $Y(s)$ is positive real [15, 16]. A real-rational function $G(s)$ is *positive real* if $G(s)$ is analytic and $\text{Re}(G(s)) \geq 0$ in $\text{Re}(s) > 0$.

3. Problem formulation

3.1. General notation

The set of natural, real and complex numbers is denoted by \mathbb{N} , \mathbb{R} , \mathbb{C} , respectively. $\mathbb{R}^{m \times n}$ is the set of m by n real matrices. \mathbb{R}_+ is the set of non-negative numbers and \mathbb{C}_+ is the closed right-half plane. \mathcal{H}_∞ is the standard Hardy space on the right-half plane and $\|\cdot\|_\infty$ represents the \mathcal{H}_∞ -norm.

3.2. Chain model

For a multi-storey building model, we consider a chain of N identical masses m connected by identical passive mechanical networks (Fig. 1). Each passive mechanical network provides an equal and opposite force on each mass and is assumed here to have negligible mass. A movable point $x_0(t)$ represents an earthquake displacement and the displacement of the i th mass is denoted by $x_i(t)$, $i \in \{1, 2, \dots, N\}$. We assume that the initial conditions of the movable point and the mass displacements are all zero.

The equations of motion in the Laplace transformed domain are

$$\begin{aligned} ms^2 \hat{x}_i &= sY(s)(\hat{x}_{i-1} - \hat{x}_i) + sY(s)(\hat{x}_{i+1} - \hat{x}_i) & \text{for } i = 1, \dots, N-1, \\ ms^2 \hat{x}_N &= sY(s)(\hat{x}_{N-1} - \hat{x}_N) \end{aligned}$$

where $\hat{\cdot}$ denotes the Laplace transform. In matrix form this can be written as

$$ms^2 \hat{x} = sY(s)H_N \hat{x} + sY(s)e_1 \hat{x}_0$$

and hence

$$\hat{x} = (h(s)I_N - H_N)^{-1}e_1 \hat{x}_0 \quad (1)$$

where I_N is the $N \times N$ identity matrix,

$$h(s) = sZ(s)m, Z = Y^{-1}, \hat{x} = [\hat{x}_1, \dots, \hat{x}_N]^T, e_1 = [1, 0, \dots, 0]^T \in \mathbb{R}^N,$$

$$H_N = \begin{bmatrix} -2 & 1 & 0 & \cdots & 0 \\ 1 & -2 & 1 & \ddots & \vdots \\ 0 & \ddots & \ddots & \ddots & 0 \\ \vdots & \ddots & 1 & -2 & 1 \\ 0 & \cdots & 0 & 1 & -1 \end{bmatrix} \in \mathbb{R}^{N \times N}.$$

Let us consider the characteristic polynomials d_i of $H_i \in \mathbb{R}^{i \times i}$ in the variable h given by

$$d_i = \det(hI_i - H_i) \quad (2)$$

Then $d_1 = h + 1$. Suppose also $d_{-1} = 1$ and $d_0 = 1$. Using the Laplace expansion of (2), we find that $d_i(h) = (h + 2)d_{i-1}(h) - d_{i-2}(h)$ for $i = 1, \dots, N$. Equation (1) can be written using d_i as

$$\hat{x} = \frac{\text{adj}(h(s)I_N - H_N)}{\det(h(s)I_N - H_N)}e_1 \hat{x}_0 = \frac{1}{d_N} \begin{bmatrix} d_{N-1} & * & \cdots \\ \vdots & \vdots & \\ d_0 & * & \cdots \end{bmatrix} \begin{bmatrix} 1 \\ 0 \\ \vdots \\ 0 \end{bmatrix} \hat{x}_0 = \begin{bmatrix} d_{N-1}/d_N \\ \vdots \\ d_0/d_N \end{bmatrix} \hat{x}_0.$$

Then the intermass displacement of the i th mass defined by $\delta_i = x_i - x_{i-1}$ in the Laplace domain is given by $\hat{\delta}_i = ((d_{N-i} - d_{N-i+1})/d_N) \hat{x}_0 =: T_{\hat{x}_0 \rightarrow \hat{\delta}_i} \hat{x}_0$ for $i = 1, \dots, N$.

We will say that the system of Fig. 1 is *stable* if all poles in the transfer functions $T_{\hat{x}_0 \rightarrow \hat{\delta}_i}$ have negative real parts in the s -domain. The following theorem gives an explicit condition for stability:

Theorem 1 ([13]). *For $0 \neq Z(s)$ positive real, the system of Fig. 1 is stable if $sZ(s)m$ does not take values in the interval $(-4, 0)$ for any s with $\text{Re}(s) = 0$.*

Table 1. Vibration control device layouts.

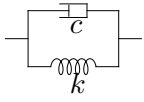
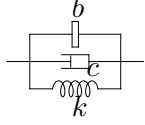
L1	L2
$Y(s) = c + \frac{k}{s}$	$Y(s) = bs + c + \frac{k}{s}$
	

Table 2. Parameters of vibration control devices.

	Layout	c (kNs/m)	b (kg)
Device 1	L1	4.0×10^3	–
Device 2	L1	6.0×10^3	–
Device 3	L2	6.0×10^3	1.0×10^5

3.3. Intermass displacements

The transfer functions from the disturbance to a given intermass displacement in a chain of N masses are represented in the form of complex iterative maps.

Theorem 2 ([13]). *For any $i = 1, 2, \dots$, intermass displacements in a chain of N masses satisfy the recursion:*

$$-T_{\hat{x}_0 \rightarrow \hat{\delta}_i} =: F_N^{(i)} = \frac{d_{i-2}F_{N-1}^{(i)} + h}{F_{N-1}^{(i)} + d_i} \quad (3)$$

for $N = i, i+1, \dots$, where $T_{\hat{x}_0 \rightarrow \hat{\delta}_i}$ is the transfer function from the disturbance x_0 to the i th intermass displacement δ_i , $F_{i-1}^{(i)} = 0$, $h(s) = sZ(s)m$ and d_i is as defined in (2).

The above recursion describes a sequence of transfer functions in the complex variable s . It can also be interpreted as a complex iterative map [17] for a given fixed $s \in \mathbb{C}$, or equivalently a fixed $h \in \mathbb{C}$.

4. Graphical approach for an arbitrary length mass chain

For the purpose of graphical representations we now introduce the inverse of h :

$$g(s) = h^{-1}(s) = Y(s)/(sm). \quad (4)$$

Fig. 2 shows the region of the complex values of g ($= h^{-1}$) for which $\max_N |F_N^{(1)}(h)| \leq \gamma$ with $1 \leq N \leq 200$ for a positive constant γ . The spacing of the contours is 0.2 where $\ln(\gamma)$ takes the value 0, 0.2, 0.4, \dots . The outermost boundary represents $\gamma = 1$ and \mathcal{G}_1 denotes the set $\{g \in \mathbb{C} : \max_N |F_N^{(1)}(g^{-1})| \leq 1\}$. This means that $\max_N \|F_N^{(1)}(h(s))\|_\infty \leq 1$ if and only if $g(s) \in \mathcal{G}_1$ for $s \in \mathbb{C}_+$. Note that the choice of $N = 200$ is large enough to accurately determine the shape of the boundary in the figure. This is further discussed in [13].

Fig. 3 is a similar figure to Fig. 2 but shows a contour map of $\max_i \max_N |F_N^{(i)}(h)| = \gamma \in \mathbb{R}_+$ for $i = 1, 2, \dots, N$, $i \leq N \leq 200$ with the Nyquist diagrams of $g(s)$ of three passive vibration control devices. The layouts of these devices are shown in Table 1 and their structural parameters are given in Table 2. We fix the parameters of the building model as $m = 1.0 \times 10^5$ kg, $k = 1.7 \times 10^5$ kN/m (based on values given in [18]). The outermost boundary of the contours again represents $\gamma = 1$ so $\max_i \max_N \|F_N^{(i)}(h(s))\|_\infty \leq 1$ if the Nyquist diagram $g(j\omega)$ lies outside this boundary. We see that devices 2 and 3 achieve this. It is also observed that the use of the inerters improves the high frequency performance (corresponding to the origin in the g -plane). The frequency domain plots of $\max_i |F_N^{(i)}(j\omega)|$ (Figs. 4 and 5) confirm these observations.

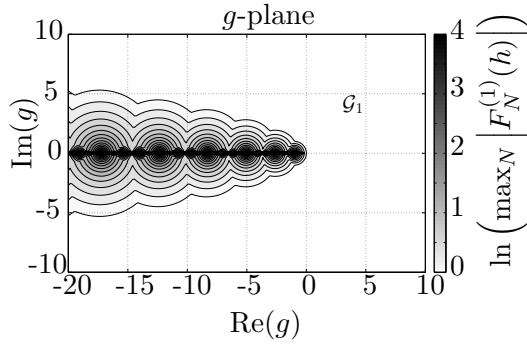


Figure 2. Contour plot of $\max_N |F_N^{(1)}(h)| = \gamma$ for $\ln(\gamma) = 0, 0.2, 0.4, \dots$ where $h = g^{-1}$.

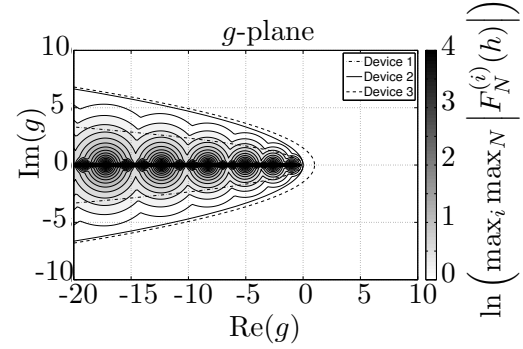


Figure 3. Nyquist diagrams of $g(s) = Y(s)/(sm)$ for the vibration control devices in Table 2 and contour plot of $\max_i \max_N |F_N^{(i)}(h)| = \gamma$ for $\ln(\gamma) = 0, 0.2, 0.4, \dots$ where $h = g^{-1}$.

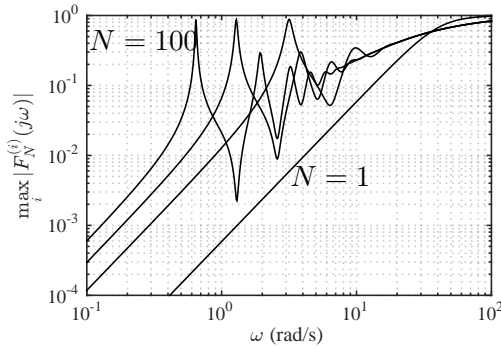


Figure 4. $\max_i |F_N^{(i)}(j\omega)|$ using Device 2 for $N = 1, 20, 50, 100$.

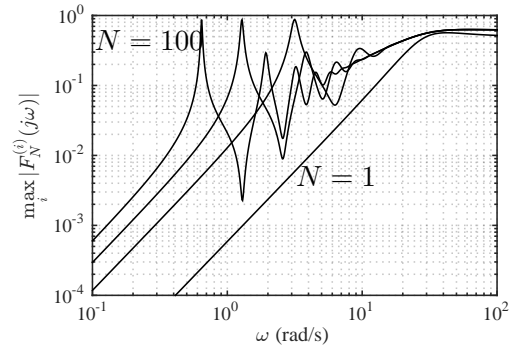


Figure 5. $\max_i |F_N^{(i)}(j\omega)|$ using Device 3 for $N = 1, 20, 50, 100$.

5. Graphical approach for a fixed length mass chain

In the previous section, a graphical approach has been introduced to design a passive interconnection which achieves a good disturbance rejection performance in an arbitrary length mass chain. In this section, we propose a design methodology for a specific length of the mass chain. The essential technique is the same as the one used for the uniform boundedness in the previous section, namely to make use of contour plots of the magnitude of the transfer functions.

As an example, we fix N as 10. Further, consider the interconnection between masses as Fig. 6 where k_s , c_s represent the storey stiffness and the structural damping. Therefore, the interconnection impedance $Z(s) = (k_s/s + c_s + Y_a(s))^{-1}$ where $Y_a(s) = Z_a(s)^{-1}$. The design task is to make the maximum value of $|F_N^{(i)}(j\omega)|$ over i small by choosing a suitable interconnection $Z_a(s)$. Using the recursions (3), one can compute the value of $\max_i |F_N^{(i)}(h)|$ at each complex value h for each N . The contour plot of $\max_i |F_N^{(i)}(h)|$ in Fig. 7 is illustrated for $N = 10$ in the g -plane where g is again the inverse of h , i.e., $g = Y(s)/(sm)$. The spacing of the contours is 0.2 where $\ln(\gamma)$ takes the value $-3, -2.8, -2.6, \dots$. The proposed design method involves essentially finding an interconnection $Y_a = Z_a^{-1}$ that moves the locus $g(j\omega)$ away from the dark region in the contour map. Since $g(s) = Y(s)/(sm) = (k_s/s + c_s + Y_a(s))/(sm)$, a large gain of $Y_a(j\omega)$ would be required especially in the frequency range where the disturbance x_0 is significant.

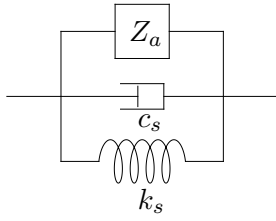


Figure 6. The layout of the interconnection Z in Fig. 1 where its admittance $Y(s) = k_s/s + c_s + Y_a(s)$ ($Y_a(s) = Z_a(s)^{-1}$).

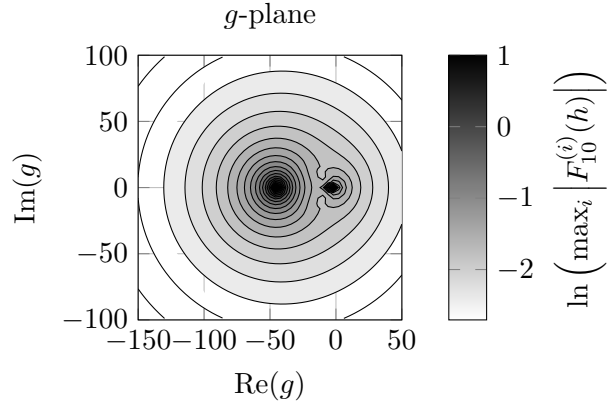


Figure 7. Contour plot of $\max_i |F_{10}^{(i)}(h)|$ where $h = g^{-1}$.

5.1. Frequency content of ground displacements

Any information on the disturbance normally helps to improve a design. In this paper, we use a weighting function $W(s)$ based on the Clough-Penzien-Kanai-Tajimi acceleration filter [19, 20] which is a commonly used model for the frequency content of strong ground motions:

$$W(s) = \frac{W_0(s)}{\|W_0(s)\|_\infty}$$

where

$$W_0(s) = \frac{1}{s^2} W_{CP}(s) W_{KT}(s) = \frac{1}{s^2} \frac{-s^2}{s^2 + 2\eta_f \omega_f s + \omega_f^2} \frac{2\eta_g \omega_g s + \omega_g^2}{s^2 + 2\eta_g \omega_g s + \omega_g^2}.$$

We employ the values for ω_g, ω_f as $8\pi, 0.8\pi$ (rad/s) respectively and both η_g, η_f as 0.60 [21] for the numerical examples in this paper. Hence,

$$W(s) = \frac{-30.16s - 631.7}{0.1654(s^2 + 3.016s + 6.317)(s^2 + 30.16s + 631.7)}. \quad (5)$$

6. Case Study

This section shows the design procedure proposed in the last section using a benchmark model for a 10-storey building.

6.1. Multi-storey homogeneous building model

Consider a 10-storey building model depicted in Fig. 1 ($N = 10$) with the interconnection of Fig. 6. The structural parameters are shown in Table 3. The floor mass m and the storey stiffness k_s are fixed as 1.00×10^5 kg and 1.77×10^5 kN/m and a period T_1 equal to $0.1N$ seconds is assumed for the first natural frequency ω_1 [22]. The structural damping is assumed to be stiffness-proportional damping with the damping ratio being 0.02, that is, $c_s = 2 \times 0.02 k_s / \omega_1$.

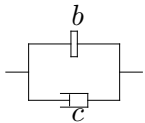
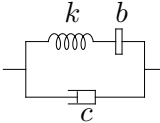
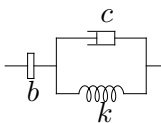
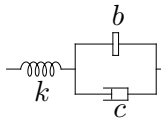
6.2. Interconnection design

For this case study, the impedance Z as in Fig. 6 is considered with Y_a being the simple interconnection configurations listed in Table 4. Note that layout L3 is called a tuned-inerter-damper (TID) in [6] and layout L4 is called a tuned viscous mass damper (TVMD) in [7, 8]. The

Table 3. Structural parameters of the homogeneous building model.

Parameter	Value	Description
N	10	Number of storeys
m	1.00×10^5 kg	Floor mass
k_s	1.77×10^5 kN/m	Storey stiffness
c_s	1.12×10^3 kNs/m	Structural damping
T_1	1.00 s	Undamped first natural period
ω_1	6.28 rad/s	Undamped first natural frequency

Table 4. Interconnection configuration and corresponding admittance $Y_a(s)$.

L1	L2	L3	L4
$bs + c$	$c + \frac{bks}{bs^2 + k}$	$\frac{bcs^2 + bks}{bs^2 + cs + k}$	$\frac{bks + ck}{bs^2 + cs + k}$
			

parameters of each element are selected making use of the contour plot of Fig. 7. For layout L1, it is clear that larger values of c push $g(j\omega)$ away from the dark region in Fig. 7. Here the value is fixed as $c = 2 \times 0.2k_s/\omega_1 = 1.12 \times 10^4$ kNs/m assuming 20 % of critical damping. As can be seen from Fig. 8a, although the inerter improves the performance in the mid to high frequency range (see the white markers \circ), it makes the low frequency performance worse (see the black markers \bullet). This is confirmed by the frequency domain plots of $\max_i |F_{10}^{(i)}(j\omega)W(j\omega)|$ in Fig. 8b.

The admittance $Y_a(s)$ of layout L2 has infinite gain at $\omega = \sqrt{k/b}$. Here this frequency is set to be the same frequency as the undamped first natural frequency of the building ω_1 . The damping coefficient is again fixed as 1.12×10^4 kNs/m. The Nyquist diagrams of $g(j\omega)$ for three values of inerter and $k = b\omega_1^2$ are drawn again on the contour plot in Fig. 9a. The larger inerter is beneficial in a broad frequency range around ω_1 which can be also seen from the frequency domain plots of $\max_i |F_{10}^{(i)}(j\omega)W(j\omega)|$ in Fig. 9b.

Similarly, layouts L3 and L4 can be designed using the contour plot of $\max_i |F_{10}^{(i)}(h)|$. The parameters given in Table 5 are an example of good design with respect to the proposed design method. Note that the inerter $b = 0$ for L1 which means L1 is just a damper with no inerter in parallel. The Nyquist diagrams of $g(j\omega)$ for each layout are illustrated in Fig. 10a. The frequency domain plots of $\max_i |F_{10}^{(i)}(j\omega)W(j\omega)|$ are also shown in Fig. 10b. Layout L1 can suppress the disturbance amplification well for the entire frequency range. The other layouts L2 – L4 improve the disturbance rejection performance around the first natural frequency ω_1 but mild peaks appear at some other frequencies.

6.3. Time response

To verify the validity of the proposed design method, this section shows the time response of the system against historical earthquakes. The interconnection configurations and their parameters

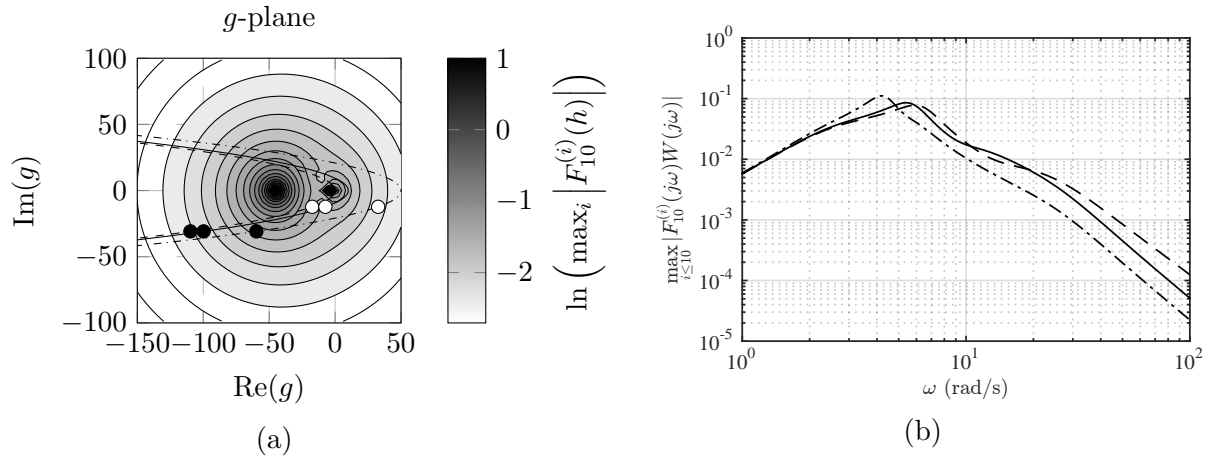


Figure 8. Design of layout L1. The parameters are: $-- c = 1.12 \times 10^4$ kNs/m, $b = 0$ kg, $— c = 1.12 \times 10^4$ kNs/m, $b = 1.0 \times 10^6$ kg, $- \cdot - \cdot c = 1.12 \times 10^4$ kNs/m, $b = 5.0 \times 10^6$ kg. (a) Nyquist diagrams of $g(s) = (k_s/s + c_s + Y_a(s))/(sm)$ and the contour plot of $\max_i |F_{10}^{(i)}(h)|$. The black and white markers \bullet, \circ indicate $g(4j)$ and $g(10j)$. (b) A log-log plot of $\max_i |F_{10}^{(i)}(j\omega)W(j\omega)|$.

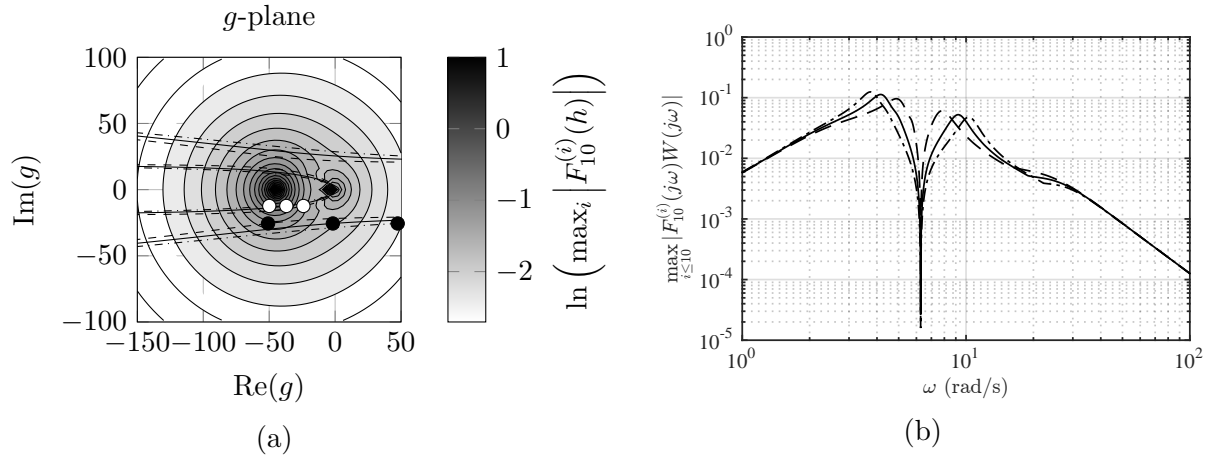


Figure 9. Design of layout L2. The parameters are: $-- c = 1.12 \times 10^4$ kNs/m, $b = 1.0 \times 10^6$ kg, $k = 3.93 \times 10^4$ kN/m, $— c = 1.12 \times 10^4$ kNs/m, $b = 3.0 \times 10^6$ kg, $k = 1.18 \times 10^5$ kN/m, $- \cdot - \cdot c = 1.12 \times 10^4$ kNs/m, $b = 5.0 \times 10^6$ kg, $k = 1.97 \times 10^5$ kN/m. (a) Nyquist diagrams of $g(s) = (k_s/s + c_s + Y_a(s))/(sm)$ and the contour plot of $\max_i |F_{10}^{(i)}(h)|$. The black and white markers \bullet, \circ indicate $g(4.7j)$ and $g(10j)$. (b) A log-log plot of $\max_i |F_{10}^{(i)}(j\omega)W(j\omega)|$.

Table 5. Parameters of vibration control devices.

Layout	c (kNs/m)	b (kg)	k (kN/m)
L1	1.12×10^4	0	—
L2	1.12×10^4	5.0×10^6	1.97×10^5
L3	1.12×10^4	5.0×10^6	1.00×10^5
L4	1.12×10^4	1.5×10^6	1.06×10^5

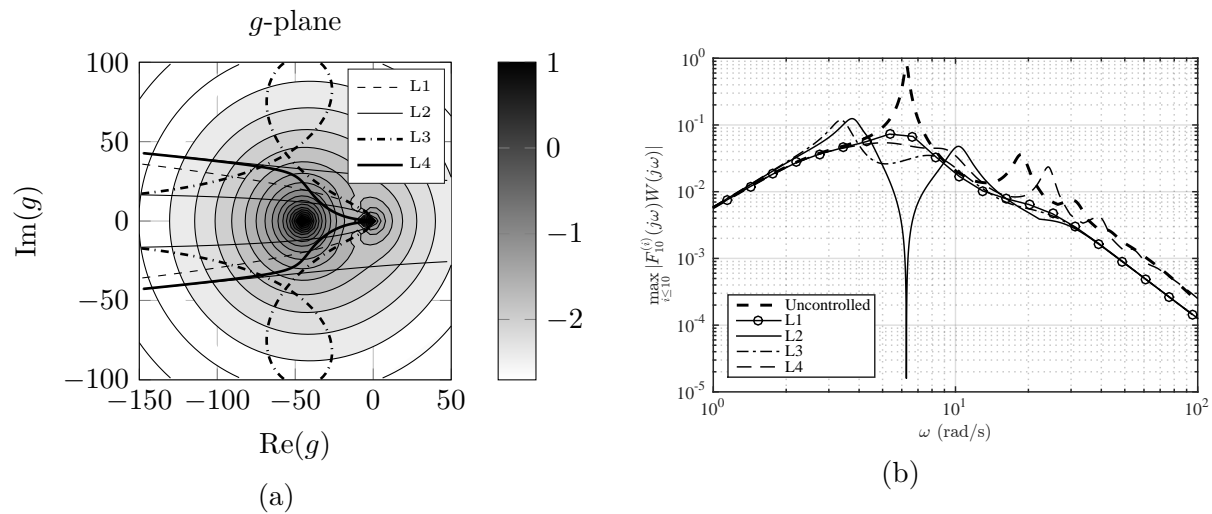


Figure 10. The design of L1 – L4 in Table 4. The parameters are given in Table 5. (a) Nyquist diagrams of $g(s) = (k_s/s + c_s + Y_a(s))/(sm)$ and the contour plot of $\max_i |F_{10}^{(i)}(h)|$. (b) A log-log plot of $\max_i |F_{10}^{(i)}(j\omega)W(j\omega)|$ for the uncontrolled homogeneous building model and the model controlled by the vibration control devices L1 – L4.

for $Y_a(s)$ designed in the previous section are listed in Table 4 and 5. The system with $Y_a(s) = 0$ is again referred to as the uncontrolled model.

Figure 11 illustrates the time response of the first interstorey drift for these four configurations against the JMA Kobe 1995 NS earthquake. All the devices L1 – L4 suppress the vibration well. The interstorey drifts are under 4 cm while the uncontrolled model experiences an interstorey drift as large as 8 cm. The vibration also attenuates much quicker than the uncontrolled model. The maximum interstorey drifts of each floor during the earthquake are shown in Fig. 12 against the JMA Kobe 1995 NS earthquake and the El Centro 1940 NS earthquake. These figures confirm that the proposed designs reduce the interstorey drifts for all the floors.

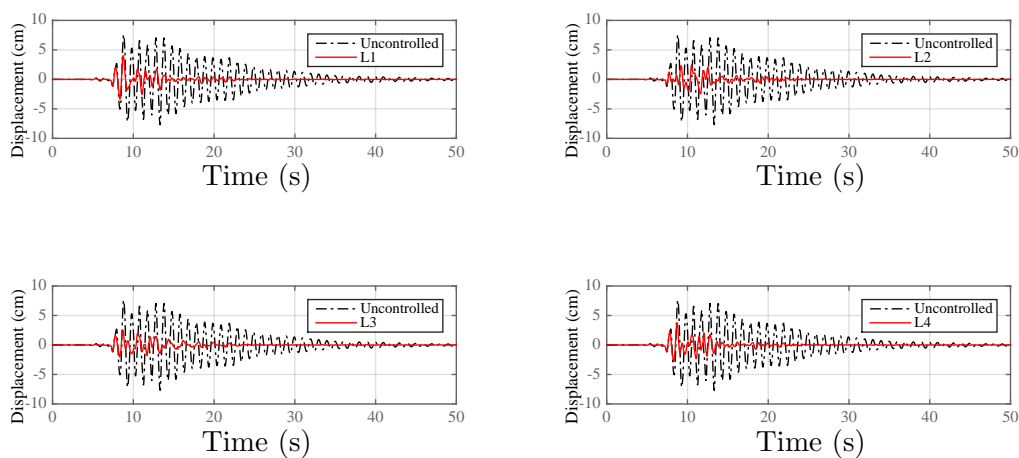
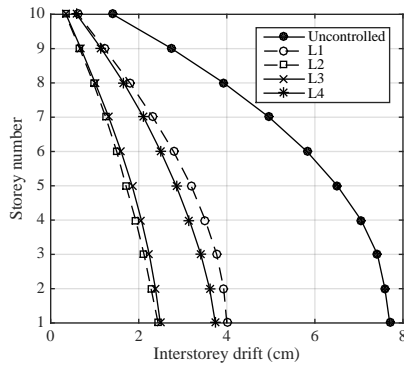
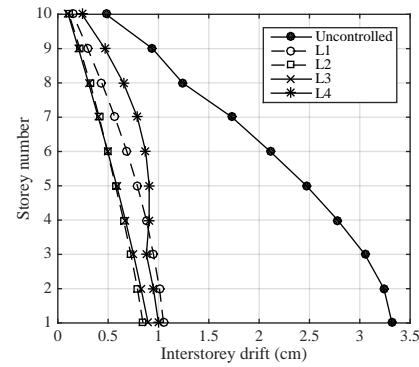


Figure 11. Time response of the first interstorey drift against the JMA Kobe 1995 NS earthquake.



JMA Kobe 1995 NS.



El Centro 1940 NS.

Figure 12. Maximum interstorey drifts against historical earthquakes for the uncontrolled homogeneous building model and the model controlled by the vibration control devices L1 – L4.

6.4. Heterogeneous mass chain model

For many tall buildings, the storey stiffness is smaller in the higher storeys. The aim of this section is to demonstrate the effectiveness of the proposed design in Table 5 for such a building when the undamped natural frequency ω_1 is the same. Consider a 10-storey building where all the masses have the same value as the homogeneous building model, i.e., $m_i = 1.00 \times 10^5$ kg, and the i th storey stiffness k_{si} for $i = 1, 2, \dots, 10$ is given by $k_{si} = \{N(N+1) - i(i-1)\}m\omega_1^2/2$ assuming that the shape of the fundamental eigenmode of the main frame is a straight line [22, 23]. The structural damping is assumed to be proportional to the stiffness with the damping ratio 0.02. Hence, $c_{si} = 2 \times 0.02k_{si}/\omega_1$ for $i = 1, 2, \dots, 10$. All the interconnections are assumed to be identical, and the layout L1 – L4 in Table 4 for the interconnection admittances with the parameters given in Table 5 are considered here. The log-log plot of $\max_i |F_{10}^{(i)}(j\omega)W(j\omega)|$ in Fig. 13 and the figure of the maximum interstorey drift of the building against the JMA Kobe 1995 earthquake in Fig. 14 confirm that the interconnections designed in the previous section give a good disturbance rejection/suppression performance.

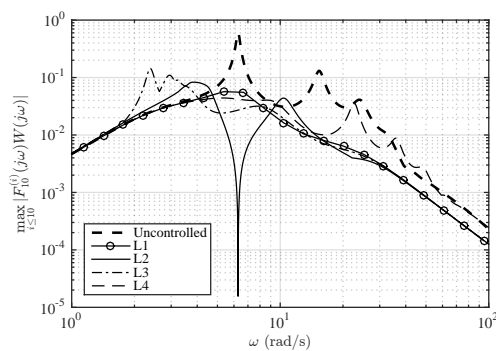


Figure 13. A log-log plot of $\max_i |F_{10}^{(i)}(j\omega)W(j\omega)|$ for the uncontrolled heterogenous building model and the model controlled by the vibration control devices L1 – L4.

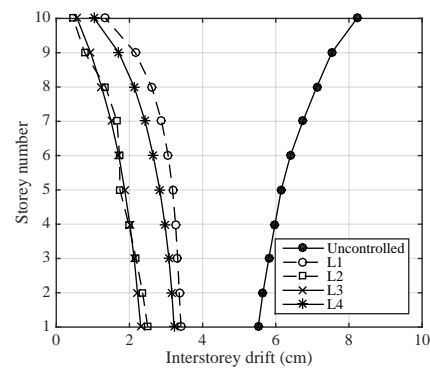


Figure 14. Maximum interstorey drift against the JMA Kobe 1995 NS earthquake for the uncontrolled heterogenous building model and the model controlled by the vibration control devices L1 – L4.

7. Conclusions

A passive vibration control problem of a multi-storey building subjected to an earthquake has been studied. A homogenous mass chain model has been considered as the building model, i.e., a chain of N identical masses in which neighbouring masses are connected by identical passive mechanical impedances, and where the first mass is also connected by the same impedance to a movable point. The transfer functions from the disturbance to inter-storey drifts have been employed as the performance measure. Two graphical design approaches have been proposed. The first approach makes use of a graph indicating the region of the complex plane for a dimensionless parameter h^{-1} to achieve a small infinity norm of these transfer functions, independent of the length of the mass chain. The second approach is for a fixed length of the mass chain. A case study has been presented to demonstrate the effect of the technique using a 10-storey building model. A method to incorporate information on the disturbance into the design is also explained. Time responses for historical earthquakes have been given to verify the effectiveness of the proposed method. The disturbance suppression performance of the designed interconnection is also verified for a heterogeneous 10-storey building model which has a different stiffness distribution but with the same undamped first natural frequency as the homogeneous model.

Acknowledgements

This work was supported in part by Funai Overseas Scholarship, by NSF under Grant ECCS-1509387 and by the AFOSR under Grants FA9550-12-1-0319 and FA9550-15-1-0045.

References

- [1] Soong T T and Dargush G F 1997 *Passive Energy Dissipation Systems in Structural Engineering* (Wiley New York)
- [2] Constantinou M C, Soong T T and Dargush G F 1998 *Passive Energy Dissipation Systems for Structural Design and Retrofit* (Multidisciplinary Center for Earthquake Engineering Research Buffalo, New York)
- [3] Takewaki I 2009 *Building Control with Passive Dampers: Optimal Performance-based Design for Earthquakes* (Wiley)
- [4] Smith M C 2002 *IEEE Trans. Automat. Contr.* **47** 1648–62
- [5] Takewaki I, Murakami S, Yoshitomi S and Tsuji M 2012 *Struct. Control. Health Monit.* **19** 590–608
- [6] Lazar I, Neild S and Wagg D 2014 *Earthq. Eng. Struct. Dyn.* **43** 1129–47
- [7] Ikago K, Sugimura Y, Saito K and Inoue N 2012 *J. Asian Archit. Build.* **11** 375–82
- [8] Ikago K, Saito K and Inoue N 2012 *Earthq. Eng. Struct. Dyn.* **41** 453–74
- [9] Marian L and Giaralis A 2014 *Probabilist. Eng. Mech.* **38** 156–64
- [10] Giaralis A and Taflanidis A A 2015 *Proc. 12th Int. Conf. Applications of Statistics and Probability in Civil Engineering* (Vancouver, Canada)
- [11] Wang F C, Chen C W, Liao M K and Hong M F 2007 *Proc. 46th IEEE Conf. Decision and Control* (IEEE) pp 3786–91
- [12] Wang F C, Hong M F and Chen C W 2010 *Proc. Inst. Mech. Eng. C J. Mech. Eng. Sci.* **224** 1605–16
- [13] Yamamoto K and Smith M C 2015 Bounded disturbance amplification for mass chains with passive interconnection (Preprint. Doi: 10.1109/TAC.2015.2478126)
- [14] Anderson B D O and Vongpanitlerd S 2006 *Network Analysis and Synthesis: A Modern Systems Theory Approach (Dover Books on Engineering)* (Dover Publications)
- [15] Brune O 1931 *Journal of Mathematical Physics* **10** 191–236
- [16] Valkenburg M E V 1960 *Introduction to Modern Network Synthesis* (Wiley) ISBN 0471899917
- [17] Devaney R 1989 *An Introduction To Chaotic Dynamical Systems, 2nd Edition (Addison-Wesley Studies in Nonlinearity)* (Westview Press)
- [18] Léger P and Dussault S 1992 *J. Struct. Eng.* **118** 1251–69
- [19] Tajimi H 1960 *Proc. 2nd World Conf. Earthq. Eng.* vol 2 (Tokyo and Kyoto, Japan) pp 781–98
- [20] Clough R W and Penzien J 1975 *Dynamics of Structures* (McGraw-Hill, Inc.)
- [21] Deodatis G 1996 *Probabilist. Eng. Mech.* **11** 149–67
- [22] Shibata A 2003 *Dynamic Analysis of Earthquake Resistant Structures (in Japanese)* 2nd ed (Morikita Publishing Co., Ltd.)
- [23] Penzien J 1960 *Proc. 2nd World Conf. Earthq. Eng.* vol 2 (Tokyo and Kyoto, Japan) pp 739–60